Lithium-zinc boro-tellurite glasses doped with La_2O_3 nano particles and embedded with silver oxide: an innovative glass matrix for applications in photonic devices

Praveen Kumar R[1], *Susheela* K. Lenkennavar[2*]

[1]Department of Physics, Bangalore University, Bengaluru, Karnataka, 560056, India.
[2]Department of Physics, Faculty of science, Bangalore University, Bengaluru, Karnataka, 560056, India.

Abstract. In the present work, using the melt quenching technique, a series of five glass samples of Lithium-Zinc boro tellurite glasses, incorporated with silver oxide and doped with Lanthanum oxide, were fabricated to analyze the influence of substituting Ag_2O and ZnO with La_2O_3 on the physical, optical, and radiation effectiveness of the produced glasses. The focus of our research is on the physical, structural, Radiation and optical properties of lithium-zinc boro-tellurite glasses, doped with La_2O_3 in amounts from 0 to 0.4 mol%, and containing a consistent Ag_2O concentration of 1 mol%. The spectral properties of the acquired glass specimens have been analysed through UV–vis absorbance data. The non-crystalline state of the synthesized glasses was validated through the XRD technique. The structural changes and the presence of borate networks (BO_3 and BO_4), tellurite networks (TeO_3 and TeO_4), and associated links were established through FTIR techniques. Our work focuses on the synthesis, characterization, of zinc oxide (ZnO) and silver oxide (Ag_2O) added glass materials for optical and radiation shielding applications. Radiation shielding properties were evaluated using the Phy-X/PSD software. Considering the measured physical parameters and the structural, optical, and shielding properties, we can say that these glasses show promise for applications in photonics, including optical amplifiers and optoelectronic devices, as well as for radiation shielding.1

1. Introduction

The research community has shown increasing interest in borotellurite glasses over the past few years for their applications in optics and photonics, primarily because they can be easily produced and shaped into the required forms [1]. The ability of nonlinear optical properties to enable one light beam to govern another is vital for diverse optoelectronic and photonic applications [2]. Glasses based on boro-tellurite that incorporate different dopants

*Corresponding author: susheelakl@bub.ernet.in

have been extensively researched due to their nonlinear optical characteristics, rendering them appropriate for uses in electro-optic modulators and ultrafast optical switches [3-5]. In the present glass system, boron acts as a network former, while lithium, zinc, and silver oxides function as network modifiers. Boron is utilized for its excellent solubility for rare-earth ions, zinc oxide improves the overall glass forming properties, and silver oxide influences the local structural layout of the glass network [6, 7]. Zinc oxide helps to maintain low crystallization rates in the glass system. Adding Li_2O as a modifier converts four-coordinated tetrahedral boron [BO_4] into three-coordinated triangular boron [BO_3], which increases the network dimensions and improves connectivity within the glass structure [8]. Gedam and Ramteke (2012) highlighted that lanthanum oxide has a remarkable ability to change the physical and optical properties of glasses and glass ceramics. Halimah et al. (2010) noted that silver doping alters the structure of the glass host, facilitating the transformation of the structural units in the tellurite networks from TeO_4 to TeO_3 [9, 10]. Lanthanum nanoparticles (La_2O_3) were used as the dopant in lithium–zinc borotellurite glasses. When these glasses were doped with Lanthanum nanoparticles and combined with silver oxide, the indirect energy band gap was found to range from 3.12 to 3.18 eV. Very few studies have been conducted to explore and reveal the characteristics of glass materials when lanthanum, which tends to diminish optical properties, and Ag, which enhances the optical properties, are incorporated into the lithium-zinc borotellurite glass system. Therefore, this research aims to provide a deeper understanding of how the integration of lanthanum nanoparticles and silver oxide into the lithium-zinc borotellurite glass system influences and modifies the optical properties of the glass system [11]. The incorporation of Ag_2O and Lanthanum nanoparticles resulted in a nonlinear variation in the optical properties of the lithium-zinc borotellurite glass system, particularly in the energy band gap with respect to composition. Again, the introduction of lanthanum oxide into lithium-zinc borotellurite glass reveals a nonlinear variation in the urbach energy of the glass system. Therefore, this study aims to identify and discuss the effects of silver oxide on the optical properties of the lanthanum zinc borotellurite glass network and also this research focuses on lanthanum, a unique element in the lanthanide category that lacks 4f electrons, to explore whether it exhibits the same extraordinary traits as other lanthanide elements that possess 4f electrons [12]. Glass is preferred over many other materials because it is transparent and non-toxic, which makes it suitable for radiation shielding applications [13].

A recent investigation on the $Li_2O–MgO–Bi_2O_3–SiO_2$ glass system was made by substituting Li_2O with Ag_2O. The study reported increases in density, structural stability, and chemical durability. Glasses with higher Ag_2O content also showed better attenuation and mechanical properties, making them suitable for radiation shielding [14]. To develop effective radiation shielding materials, borate glasses can be synthesized with heavy metal oxides such as TeO_2 or La_2O_3. Another approach is to modify the glass network by adjusting the composition of network formers and intermediates. These strategies help enhance both the shielding performance and the overall properties of the glass [15]. Previous research has largely focused on the role of various heavy metal oxides in borate and silicate glasses. This study focuses on the analysis of radiation shielding parameters, especially the mass attenuation coefficient and half value layer. The effect of La_2O_3 content on the half-value layer and mass attenuation coefficient is examined, showing that even thinner samples can offer good radiation shielding due to the high atomic number and density of silver oxide containing lanthanum nanoparticles doped glasses.

This paper presents a new melt quench synthesised lithium-zinc boro-tellurite glass system that includes lanthanum (La_2O_3) nanoparticles and silver oxide. The incorporation of La_2O_3 nanoparticles and Ag_2O significantly modifies the glass network, leading to a non-linear change in density and structural compactness. We conducted UV-visible absorption

measurements to examine the optical properties of La_2O_3-doped glass samples. Changes in the refractive index, optical band gap and Urbach energy were analysed as a function of La_2O_3 nanoparticle concentration. Lithium–zinc boro-tellurite glasses containing La_2O_3 nanoparticles and silver oxide were analysed using experimental and theoretical methods. The combined results give a clearer picture of their optical properties and radiation shielding characteristics.

2. Materials and Methods

2.1. Synthesis of Glass Samples

Lithium-zinc boro-tellurite glass was doped with lanthanum nanoparticles (La_2O_3). This doping process involved melting analytical reagent grade B_2O_3, which was added in the form of orthoboric acid (H_3BO_3), while Li_2O, TeO_2, and ZnO were the starting materials. The chemicals were uniformly blended into a fine powder in a ceramic mortar to achieve uniform homogeneity. The prepared batch was preheated in a porcelain crucible at 300 °C for 30 minutes to remove moisture, volatile components and to enhance the melting process. Subsequently, the temperature was raised to 900 °C and maintained for one hour to obtain a homogeneous melt. To ensure a consistent homogeneity and avoid bubbles in the melt, the crucibles were shaken often. The transparent melt was poured and promptly quenched between stainless steel rings. Each glass was annealed at 300 °C for 2 hours to decrease mechanical stress. After this, the furnace was switched off, allowing the samples to cool gradually to room temperature at a controlled rate of 30 °C per hour. The glasses prepared are referred to as BTLZAgLa1, BTLZAgLa2, BTLZAgLa3, BTLZAgLa4, and BTLZAgLa5, respectively.

2.2. Sample characterization

2.2.1. X-ray diffraction

The glassy state of the synthesized lithium-zinc boro tellurite glasses was examined through XRD analysis. XRD spectra obtained using a Rigaku Ultima-VI at room temperature.
The structural analysis of the building units in the prepared glasses was conducted by recording their Fourier Transform Infrared (FTIR) absorption spectra. PerkinElmer instrument was used for the measurements. The spectra were collected within the range of 400-4000 cm^{-1}.

2.2.2. Uv characteristics.

The optical (UV–Visible) absorption spectra of the polished glass samples, with an average thickness of 2.67 mm, were recorded at room across a wavelength range of 200–1800 nm. Each sample was measured twice to verify the reproducibility of the absorption peak data.

2.2.3. molar volume and density

The density (ρ) of the glass samples was measured experimentally using Archimedes' principle. Each sample was first weighed in air and then immersed in toluene. The density was calculated using the following equation (1) [16]:

$$\rho = \frac{W_A}{W_A - W_t}\,\rho_t \qquad (1)$$

here W_A is the weight of the glass measured in air, W_t is the weight of the glass sample when immersed in toluene, and ρ_t is the density of toluene at room temperature, taken as 0.865 g/cm^3. Subsequently, the molar volume (V_m) was found by dividing the average molecular weight (M) of the glass composition by its measured density (ρ). Furthermore, oxygen packing density is the measure of the compactness of the oxide network structure in oxide glasses. The OPD can be calculated using the molar volume (V_m) and the number of oxygen atoms (n) present in the glass component through the following formula (2).

$$OPD = \frac{1000 \times n}{V_m} \qquad (2)$$

3. Outcome & Scrutiny

3.1. Phase Recognition

Displayed in Fig. 1, is the XRD pattern of the BTLZAgLa glass sample, recorded within the range of $10° \leq \theta \leq 90°$. The absence of sharp diffraction peaks suggests that the samples have an amorphous structure. The extensive variations in the patterns are due to X-ray scattering in the disordered glass, which implies structural irregularities over a wide range. Thus, it is confirmed that the materials are non-crystalline and possess a glassy nature. Usually, boro tellurite glasses show a broad halo in their XRD patterns within the range of 25° to 33°.

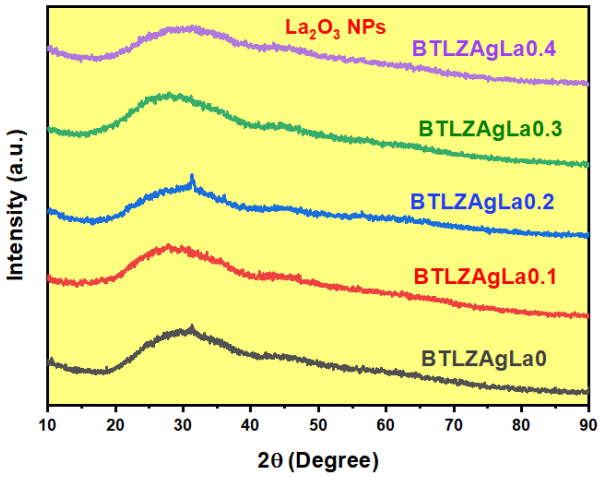

Fig. 1. XRD for La NPs Incorporated Zinc Boro-tellurite glasses.

3.2. Functional group investigation

A significant study in glass science is Fourier Transform Infrared Spectroscopy (FTIR), which is utilised to identify the functional groups present within the glass system and examine the construction units. The FTIR spectra recorded for the Lithium zinc boro-

tellurite glasses containing Lanthanum nanoparticles is clearly shown in Fig. 2. The samples were analysed within a wavelength range of 500-4000cm^{-1}. This study particularly emphasised the mid-infrared region (500-1600 cm^{-1}), where different vibrational modes related to lanthanum NPs-doped lithium-zinc boro tellurite glasses are observed.

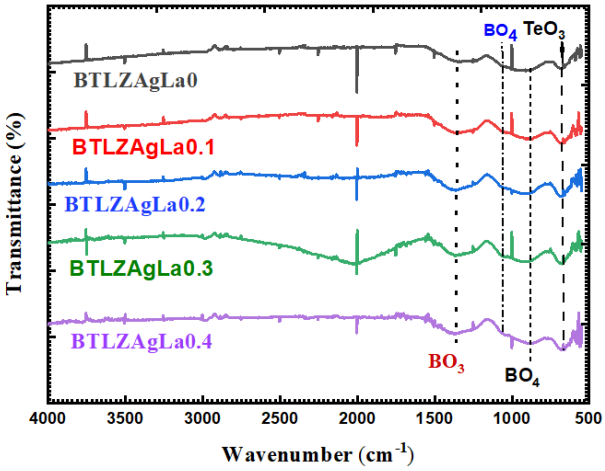

Fig. 2. FTIR spectra of lithium-zinc borotellurite glasses doped with La_2O_3 NPs.

Table 1. Assignment of infrared transmission bands of lanthanum nanoparticles doped lithium-zinc borotellurite glasses.

Wavenumber (cm^{-1})	Assignment (vibrational modes)	References
680 cm^{-1}	Formation of TeO_3 trigonal pyramidal	[16, 17]
883 cm^{-1}	B-O stretching vibrations in tetrahedral BO_4 units.	[18]
1356 cm^{-1}	Asymmetric stretching relaxation of the B-O band of trigonal BO_3 units	[19]

Generally, tellurium and boron, which function as network formers, can be present in a boro-tellurite glass system as TeO_3, BO_4, and BO_3. The molecules will vibrate at 600-650 cm^{-1}, 650-700 cm^{-1}, 800-1200 cm^{-1}, and 1200–1400 cm^{-1}, respectively, after they absorb infrared radiation [13, 17, 20]. The suitable assignments for Lanthanum nanoparticles doped Lithium-zinc Boro-tellurite glasses are listed in Table 1. The band noted around 883 cm^{-1} corresponds to di-borate units and B-O-B linkages in the borate structure. Asymmetrical stretching of B-O vibrations causes a band to appear at 1356 cm^{-1}. The absence of an absorption band for ZnO and La_2O_3 in the FTIR spectra indicates that the zinc and lanthanum lattices are completely broken down [18].

3.3. Physical properties

3.3.1. density and molar volume

The density (ρ), molar volume (V_m), and oxygen packing density (OPD) of the prepared glasses were calculated using standard formulas and are shown in Table 2. These

parameters play a significant role in the investigation of structural changes. Various factors, such as coordination number, network structure, cross-link density, and interstitial spaces, impact these properties.

Table 2. Density (ρ) and molar volume (V_m) and Oxygen packing density parameter of the glass samples.

La_2O_3 (mol%)	Density (g/cm^3)	Molar Volume (cm^3/mol)	OPD (g-atm/l)
0	2.9124	24.49182805	326.6395626
0.1	2.9261	24.4694303	449.5405028
0.2	2.9187	24.62397643	446.7190761
0.3	2.9467	24.48162351	449.3166066
0.4	2.9345	24.67882092	445.7263187

Fig. 3 shows the relationship between ρ and V_m as a function of La_2O_3 mol%, and the corresponding values for the prepared glass compositions are given in Table 2. The density of the glass samples lies between 2.912 and 2.9345 g cm^{-3}. The small increase in density with changing composition results from the addition of heavier modifier ions, which create a denser glass structure and improve atomic packing within the network. The slight decrease in density is also observed for specific compositions at 0.2 mol% and 0.4 mol%. This decrease can be explained by an increase in molar volume arising from structural rearrangements in the glass network. In general, the molar volume (V_m) of a glass is inversely related to its density. In our glass samples, an inverse relationship between density and molar volume is observed across all compositions.

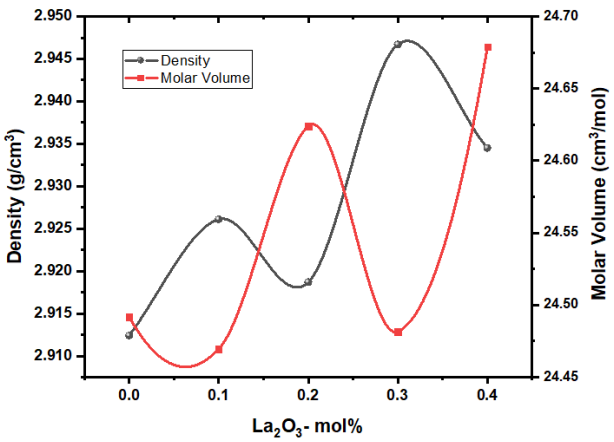

Fig. 3. Variation of density and molar volume with La_2O_3 (mol%).

3.4. Optical characteristics

UV-visible spectroscopy serves as an effective method for exploring the optical properties of materials, including band gaps and Urbach energies. Fig. 4 displays the UV-visible diffuse absorbance spectra of the analysed glass samples.

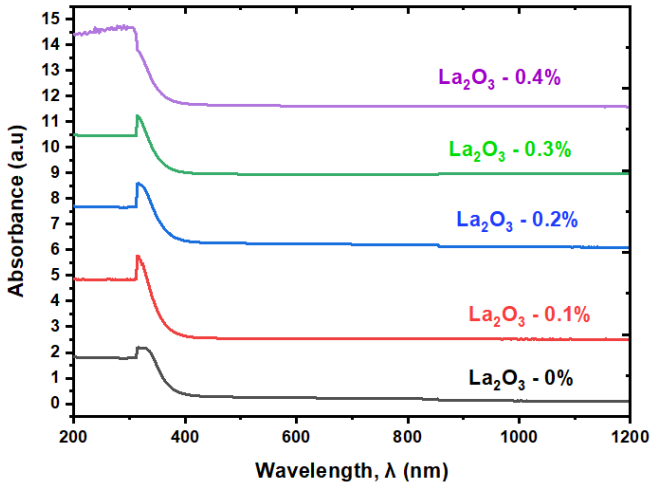

Fig. 4. Optical absorption spectra for the prepared Lithium zinc boro-tellurite glass samples.

The absorption edge ranges widely from 320 to 400 nm in the base glass, highlighting the amorphous nature of the prepared samples. Below 320 nm, the spectra indicate a saturation region, and beyond 320 nm, there is a decrease in absorption, which corresponds to transitions from the valence band to the conduction band [21]. Optical transitions are not seen in the visible region. This is because there are no partially filled d orbitals available to support d–d electronic transitions, given that the ions like Ag^{+} and Zn^{2+} have filled d^{10} electronic configurations. Moreover, network formers such as B_2O_3 and TeO_2 do not facilitate d–d transitions. The optical spectra observed in non-crystalline materials often consist of three distinct regions: (i) a phonon-assisted constant absorption region, (ii) the Tauc region, which corresponds to strong absorption caused by inter-band electronic transitions, and (iii) the Urbach region, where the absorption coefficient has an exponential relationship with photon energy [22].

3.4.1. Energy Band gap

The optical band gap indicates the energy difference between the maximum of the valence band and the minimum of the conduction band. For amorphous materials, the calculation can be performed using models derived from the Tauc method, initially introduced by Davis and Mott, and represented by the following equation [23, 24].

$$\alpha h\upsilon = q\,(h\upsilon - E_g)^m \qquad (3)$$

Where hυ signifies the energy of the photon, q is a constant, E_g is the optical band gap, m refers to an index that can take on different values (1/2 for indirect transitions and 2 for direct allowed transitions), and α is the absorption coefficient.

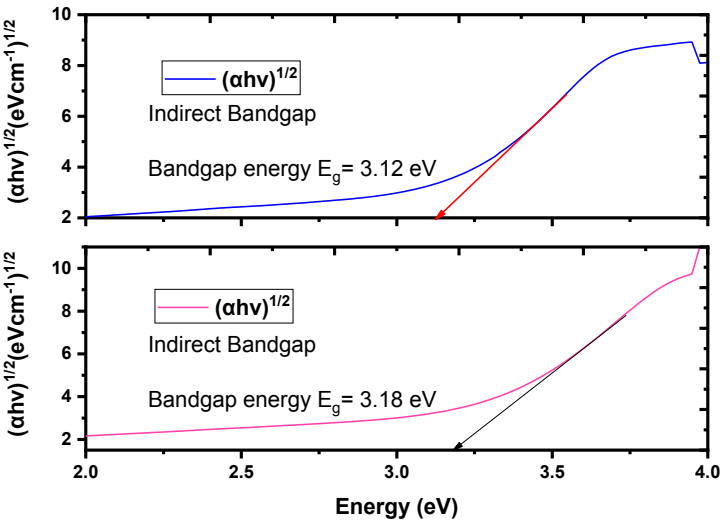

Fig. 5. Part of indirect band gap graph $(\alpha hv)^{1/2}$ in prepared glass.

Fig. 5, displays the E_g Values (indirect band gap) associated with the prepared glass samples. The indirect band gap values, Urbach energy, and refractive index values are summarised in Table 3, highlighting a non-linear variation in relation to the concentration of La_2O_3 nanoparticles.

Table 3. Eg , ΔE and Refractive index of lithium-zinc borotellurite glasses doped with lanthanum nanoparticles.

La_2O_3 (mol%)	Indirect energy band gap, E_g (eV)	Urbach energy, ΔE (eV)	Refractive Index (R.I)
0	3.12	0.288	2.36
0.1	3.16	0.297	2.35
0.2	3.12	0.284	2.36
0.3	3.22	0.272	2.34
0.4	3.18	0.320	2.35

The presence of bridging oxygen in the glassy matrix is responsible for the increase in E_g values [25]. Thus, the introduction of La_2O_3 NPs into the glass network has hindered the flow of electrons within the synthesised materials [26]. The indirect optical band gap of the synthesised glass samples ranges from 3.12 to 3.18 eV, demonstrating their wide band gap characteristics and excellent optical transparency. The non-linear change in E_g with varying La_2O_3 concentration is due to the competing influences of non-bridging oxygen formation and network reorganisation. At intermediate levels of La_2O_3, there is an increase in E_g due to structural compactness. The considerable drop in the energy band gap value may be due to a significant structural change that occurred in the glass system of the glass sample with a 0.3 molar fraction of La_2O_3 NPs. Urbach energy (ΔE) values are calculated from the slopes of the linear sections of the ln α versus hv plots. An observable decrease in ΔE occurs as the amount of La_2O_3 NPs in the glass system increases at 0.2 mol% and 0.3 mol%. This downward trend in ΔE is linked to a reduction in the number of defects present in the glass matrix.

Defects present in the glass network, such as an increasing number of non-bridging oxygen and cation-anion vacancy pairs, could explain the increase in the ΔE value at a 0.4 molar fraction of La_2O_3 nano particles [27]. Refractive Index: Table 3 provides the specific values of the refractive index. The relationship and understanding of the refractive index can be enhanced by analysing the formation of bridging and non-bridging oxygen in a substance. The findings of this research indicate that with a higher amount of La_2O_3 nanoparticles, there is a decreasing trend in the refractive index, which is attributed to the presence of low-polarizability bridging oxygen in the glass network. Simultaneously, the structural alterations that take place at 0.2 and 0.4 molar fractions of La_2O_3 nanoparticles resulted in a marked increase in nonbridging oxygen formation. Nonbridging oxygen is responsible for creating more ionic bonds, which display a higher polarizability than the mainly covalent bonds associated with bridging oxygen. As a result, a greater refractive index value is observed when nonbridging oxygen is present in larger quantities than bridging oxygen within the material [28].

3.5. Gamma radiation attenuation properties

The mass attenuation coefficient (μ_m), as seen in Fig. 10, and the half value layer (HVL), as illustrated in Fig. 6, were examined for the synthesised lithium-zinc borotellurite glass composites with different La_2O_3 concentrations over the energy range of 0.015-15 MeV. It is clear that when the γ photon attains 1 MeV, the MAC values drop rapidly. This reduction is due to photoelectric absorption. This effect is particularly important at lower photon energy levels. Therefore, the MAC values for the glasses being studied and the materials being compared are highest in the low energy range. The analysis demonstrated that the highest MAC values for all BTLZAgLa samples were found at 0.015 MeV, with a subsequent sharp decrease as photon energy increased. At 0.015 MeV, the MAC values are 23.369 cm^2/g and 23.846 cm^2/g for La_2O_3 at 0 mol% and 0.4 mol% respectively.

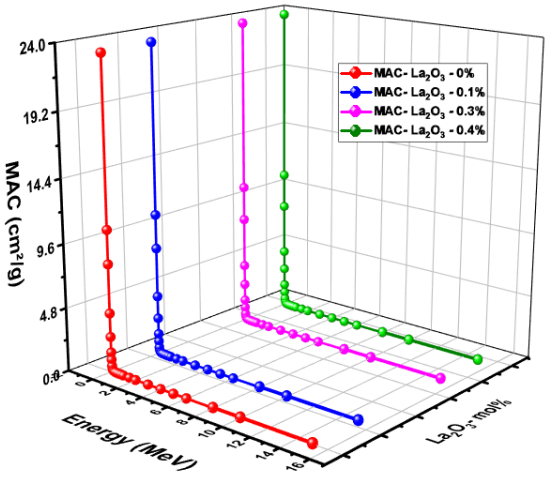

Fig. 6. Mass attenuation coefficients (μ/ρ) of the investigated glasses as a function of the photon energy-La_2O_3 incorporated glasses.

The HVL of BTLZAgLa glass is illustrated in Fig. 7, as a function of energy. A significant metric for any shielding material is the HVL, which is the thickness required to reduce the photon-beam intensity by half as it passes through the material. Therefore, selecting lower values is advisable for identifying the most effective γ-ray shielding composition. For

La_2O_3-0.4% glass, the HVL value was found to be 4.750 cm at 1.5 MeV, The lowest HVL value of La_2O_3-0.4% glass highlights its superior shielding capabilities compared to all other glasses produced.

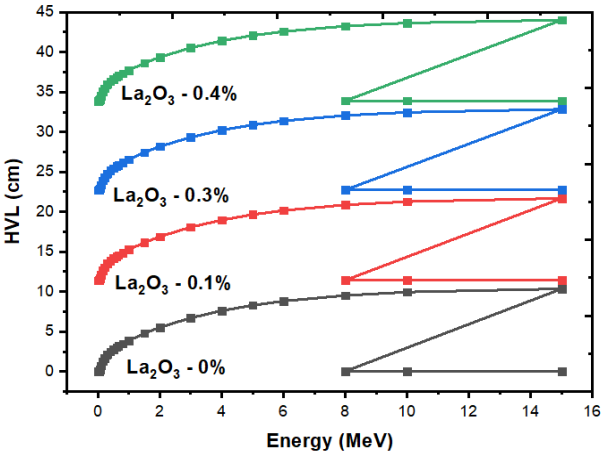

Fig.7. half-value layers versus incident photon energy

4. Conclusion

Lithium-zinc borotellurite glasses infused with lanthanum oxide nanoparticles have been successfully created. The structural, physical, radiation and optical characteristics of the produced samples were thoroughly examined and documented. The broad hump observed in the XRD diffraction pattern validated the amorphous nature of the samples. The declining trend in urbach energy values indicates that the glasses fabricated are less fragile. The pattern variations at 0.3 and 0.4 molar fractions of La_2O_3 nanoparticles for urbach energy and refractive index are attributed to structural changes in the glass system, which lead to a greater formation of non-bridging oxygen.

The results indicate that the highest MAC values were observed at an energy of 0.015 MeV for all the prepared glasses. The results indicate that the BTLZAgLa0.4% glass has the lowest HVL. Therefore, the evaluation of shielding characteristics implies that BTLZAgLa0.4% glass provides superior gamma radiation shielding compared to other traditional materials. The results show that lithium-zinc borotellurite glass doped with lanthanum nanoparticles and containing silver oxide has a higher refractive index than conventional silicate glass, which is commonly used for optical fibers. This implies that rare-earth doped borotellurite glass could be an effective material for optoelectronics and photonics applications. Lithium-zinc borotellurite glasses doped with La_2O_3 nanoparticles and silver oxide show notable optical and radiation shielding capabilities, positioning them as promising options for rare-earth-doped optical glasses, optoelectronic applications, and radiation protection.

Acknowledgement

The authors acknowledge financial support from the Vision Group on Science and Technology (VGST), Government of Karnataka, under KSTEPS/VGST/ECRA/GRD No. 1251/2023-24.

References

1. S. P. Singh and B. Karmakar, Photoluminescence enhancement of Eu^{3+} by energy transfer from Bi^{2+} to Eu^{3+} in bismuth glass nanocomposites. RSC Advances 1, 751 (2011). https://doi.org/10.1039/C1RA00160D
2. H. Nasu, J. Matsuoka, O. Sugimoto, M. Kida, and K. Kamiya, Non-Resonant Type Third-Order Optical Nonlinearity of Rare Earth Oxides-Containing GeO_2 Glasses:optical materials and their applications. Journal of the Ceramic Society of Japan. 101, 43-47 (1993). https://doi.org/10.2109/jcersj.101.43
3. A. S. Asyikin, M. K. Halimah, A. A. Latif, M. F. Faznny, and S. N. Nazrin, Physical, structural and optical properties of bio-silica borotellurite glass system doped with samarium oxide nanoparticles. Journal of Non-Crystalline Solids. 529, 119777 (2019). https://doi.org/10.1016/j.jnoncrysol.2019.119777
4. M. R. Zaki, D. Hamani, M. Dutreilh-Colas, J.-R. Duclère, J. De Clermont-Gallerande, T. Hayakawa, O. Masson, and P. Thomas, Structural investigation of new tellurite glasses belonging to the TeO_2-$NbO_2.5$-WO_3 system, and a study of their linear and nonlinear optical properties. Journal of Non-Crystalline Solids. 512, 161 (2019). https://doi.org/10.1016/j.jnoncrysol.2019.02.027
5. L. Y. Mao, J. L. Liu, L. X. Li, and W. C. Wang, TeO_2-Ga_2O_3-ZnO ternary tellurite glass doped with Tm^{3+} and Ho^{3+} for 2μm fiber lasers. Journal of Non-Crystalline Solids. 531, 119855 (2019). https://doi.org/10.1016/j.jnoncrysol.2019.119855
6. H. Lin, E. Y.-B. Pun, X. Wang, and X. Liu, Intense visible fluorescence and energy transfer in Dy^{3+}, Tb^{3+}, Sm^{3+} and Eu^{3+} doped rare-earth borate glasses. Journal of Alloys and Compounds. 390, 197 (2004). https://doi.org/10.1016/j.jallcom.2004.07.068
7. A. Usman, H. MK, A. A. Latif, F. D. Muhammad, and A. I. Abubakar, Influence of Ho^{3+} ions on structural and optical properties of zinc borotellurite glass system. Journal of Non-Crystalline Solids. 483, 18 (2018). https://doi.org/10.1016/j.jnoncrysol.2017.12.040
8. N. S. Prabhu, V. Hegde, A. Wagh, M. I. Sayyed, O. Agar, and S. D. Kamath, Physical, structural and optical properties of Sm^{3+} doped lithium zinc alumino borate glasses. Journal of Non-Crystalline Solids. 515, 116 (2019). https://doi.org/10.1016/j.jnoncrysol.2019.04.015
9. R. S. Gedam and D. D. Ramteke, Synthesis and characterization of lithium borate glasses containing La_2O_3. Transactions of the Indian Institute of Metals. 65, 31 (2011). https://doi.org/10.1007/s12666-011-0107-4
10. M. K. Halimah, W. M. Daud, H. A. A. Sidek, A. W. Zaidan, and A. S. Zainal, Optical properties of ternary tellurite glasses. Mater. Sci. Pol. 28, 173 (2010).
11. M. F. Faznny, H. M. Kamari, A. A. Latif, F. D. Muhammad, and L. Hasnimulyati, Optical properties of La^{3+} NPs/Ag^{+} co-doped zinc borotellurite glass. Solid State Phenomena. 290, 3 (2019).https://doi.org/10.4028/www.scientific.net/SSP.290.3
12. F. M. Fudzi, H. M. Kamari, A. A. Latif, and A. M. Noorazlan, Linear Optical Properties of Zinc Borotellurite Glass Doped with Lanthanum Oxide Nanoparticles for Optoelectronic and Photonic Application. Journal of Nanomaterials. 2017, 1 (2017). https://doi.org/10.1155/2017/4150802
13. N. Almousa, S. A. M. Issa, A. S. Abouhaswa, and H. M. H. Zakaly, Improved radiation shielding efficiency and optical properties of borate glass by incorporating dysprosium(III) oxide. Materials Today Communications. 39, 109198 (2024). https://doi.org/10.1016/j.mtcomm.2024.109198
14. M. M. Ebrahium, H. A. Abo-Mosallam, M. I. Abdelglil, and K. A. Aly, Performance improvement of mechanical, chemical and radiation protection of Ag^{+}-doped bismuth

silicate glasses for radiation shielding applications. Annals of Nuclear Energy. 222, 111554 (2025). https://doi.org/10.1016/j.anucene.2025.111554
15. P. N. Patil, M. Manjunatha, M. M. Hosamani, A. S. Bennal, and N. M. Badiger, Influence of PbO_2 and Gd_2O_3 on the gamma-ray shielding performance of borosilicate glasses. Nexus of Future Materials. 2, (2025). https://doi.org/10.70128/617892
16. A. M. Noorazlan, H. M. Kamari, S. O. Baki, and D. W. Mohamad, Green emission of tellurite based glass containing erbium oxide nanoparticles. Journal of Nanomaterials. 2015, (2015). http://dx.doi.org/10.1155/2015/952308
17. M. K. Halimah, A. A. Awshah, A. M. Hamza, K. T. Chan, S. A. Umar, and S. H. Alazoumi, Effect of neodymium nanoparticles on optical properties of zinc tellurite glass system. Journal of Materials Science Materials in Electronics. 31, 3785 (2020). https://doi.org/10.1007/s10854-020-02907-9
18. S.S. Hajer, M.K. Halimah, Z. Azmi, M.N. Azlan, Optical properties of zinc borotellurite doped samarium. Chalcogenide Lett. 11 (11) (2014) 553–566.
19. A. K. Singh, C. Gautam, A. Madheshiya, V. K. Mishra, N. Ahmad, and R. Trivedi, Effect of La_2O_3 concentration on structural, optical and cytotoxicity behaviours of strontium titanate borosilicate glasses. Journal of Non-Crystalline Solids. 481, 176 (2017). https://doi.org/10.1016/j.jnoncrysol.2017.10.049
20. Kh. S. Shaaban and E. S. Yousef, Optical properties of Bi_2O_3 doped boro tellurite glasses and glass ceramics. Optik. 203, 163976 (2019). https://doi.org/10.1016/j.ijleo.2019.163976
21. A. Kh. Helmy, E. Salama, M. A. Azooz, F. H. Elbatal, M. A. Ouis, and E. E. Elshereafy, Optical, structural, and gamma shielding characteristics of bismuth-doped lithium borosilicate glass composite. Scientific Reports. 15, 38106 (2025).https://doi.org/10.1038/s41598-025-23089-6
22. A. K. Sandhu, N. Singh, and R. Kaur, Structural and optical properties of bismuth borosilicate glasses: Effect of CeO_2 doping. Applied Physics A. 130, (2024). https://doi.org/10.1007/s00339-024-07490-y
23. E. A. Davis and N. F. Mott, Conduction in non-crystalline systems V. Conductivity, optical absorption and photoconductivity in amorphous semiconductors. Philosophical Magazine. 22, 0903 (1970). https://doi.org/10.1080/14786437008221061
24. Sadeq and H. Y. Morshidy, Effect of samarium oxide on structural, optical and electrical properties of some alumino-borate glasses with constant copper chloride. Journal of Rare Earths. 38, 770 (2019). https://doi.org/10.1016/j.jre.2019.11.003
25. M. S. Malik and C. A. Hogarth, Some optical properties of TeO_2-CuO-Lu_2O_3 glasses. Journal of Materials Science Letters. 8, 655 (1989). https://doi.org/10.1007/BF01730433
26. Z. A. Talib, W. M. Daud, E. Z. M. Tarmizi, H. A. A. Sidek, and W. M. M. Yunus, Optical absorption spectrum of Cu_2O–CaO–P_2O_5 glasses. Journal of Physics and Chemistry of Solids. 69, 1969 (2008). https://doi.org/10.1016/j.jpcs.2008.02.005
27. A. Azuraida, M. K. Halimah, C. A. C. Azurahanim, and M. Ishak, Gamma irradiation effect on structural and optical properties of bismuth-boro-tellurite glasses. Advanced Materials Research. vol. 1107, pp. 426–431, 2015.
28. Y. B. Saddeek, K. A. Aly, A. Dahshan, and I. M. El. Kashef, Optical properties of the Na_2O–B_2O_3–Bi_2O_3–MoO_3 glasses. Journal of Alloys and Compounds. 494, 210 (2009). https://doi.org/10.1016/j.jallcom.2009.11.123